J. Chem. Sci. (2020) 132:112
https://doi.org/10.1007/s12039-020-01818-w

REGULAR ARTICLE

Experimental and theoretical insights on the adsorption and inhibition mechanism of (2E)-2-(acetylamino)-3-(4-nitrophenyl) prop-2-enoic acid and 4-nitrobenzaldehyde on mild steel corrosion

N ARROUSSE[a], R SALIM[a], G AL HOUARI[b], F EL HAJJAJI[a,*], A ZARROUK[c], Z RAIS[a], M TALEB[a], DHEERAJ SINGH CHAUHAN[d,*] and M A QURAISHI[d]

[a]Engineering Laboratory of Organometallic, Molecular Materials and Environment, Faculty of Sciences, University Sidi Mohamed Ben Abdellah, Fez, Morocco
[b]Laboratory of Organic Chemistry, Faculty of Sciences, University Sidi Mohamed Ben Abdellah, Fez, Morocco
[c]Laboratory of Materials, Nanotechnology and Environment, Department of Chemistry Faculty of Sciences, Mohamed V University, Rabat, Morocco
[d]Center of Research Excellence in Corrosion, King Fahd University of Petroleum and Minerals, Dhahran 31261, Saudi Arabia
E-mail: dheeraj.chauhan.rs.apc@itbhu.ac.in; el.hajjajifadoua25@gmail.com

MS received 11 April 2020; revised 18 June 2020; accepted 18 June 2020; published online 19 August 2020

Abstract. (2E)-2-(acetylamino)-3-(4-nitrophenyl)prop-2-enoic acid (NPP) was synthesized following a facile chemical method from 4-nitrobenzaldehyde (NB) and thoroughly characterized using spectroscopic techniques. These compounds were applied as novel inhibitors for corrosion of mild steel in 1M HCl using various methods such as absorbance difference, potentiodynamic polarization, and electrochemical impedance spectroscopy (EIS). The results indicate that these inhibitors show an excellent protection performance and achieve the corrosion inhibition efficiency values of 94% and 84% for NPP and NB, respectively. The adsorption of these molecules obeys the El-Awady isotherm model. The surface analysis of mild steel was investigated using scanning electron microscopy (SEM) and energy dispersive X-ray (EDX) methods. Furthermore, quantum chemical calculations were investigated using DFT method at B3LYP/6-31G (d,p) computed by Gaussian 09 showing a good correlation with the experimental results.

Keywords. Absorbance difference; DFT; EIS; polarization curves; mild steel.

1. Introduction

Depending on the engineer's point of view, corrosion is a degradation of material or its properties by chemical reaction with the environment.[1,2] This definition recognizes that corrosion is a harmful phenomenon: it destroys the material or reduces its properties, making it unusable for an intended application.[3] Therefore, several researchers are focused on this problem using different techniques to achieve high protection of materials.[4] Moreover, owing to the excellent mechanical properties and low cost of the mild steel, it is considered as a preferred structural material in various industries. However, the use of mineral acids in high concentrations, such as that used during industrial acid pickling/acid cleaning processes, causes severe corrosion of mild steel. Compared to the commonly used inorganic corrosion inhibitors, the use of low toxicity organic corrosion inhibitors is preferred in industries.[6,10–13] The use of organic inhibitors is one of the most commonly used methods in this field, especially in the acidic medium.[2,5,6] These inhibitors adsorb firstly on the surface of metals and intervene in the reaction processes of corrosion to reduce the corrosion rate.[1,2]

The benzaldehyde derivatives are widely used as corrosion inhibitors, especially in acidic medium. For example, Kumar Singh *et al.,* [7,8] studied the inhibition

*For correspondence

Electronic supplementary material: The online version of this article (https://doi.org/10.1007/s12039-020-01818-w) contains supplementary material, which is available to authorized users.

effect of 4(N,N-dimethylamino) benzaldehyde nicotinic hydrazone in 1M HCl, and it revealed excellent protective behavior against mild steel corrosion. Also, Zhang *et al.,* [9] recently synthesized and evaluated the inhibition effect of novel benzaldehyde derivatives against corrosion of mild steel, and obtained satisfactory results. In this context, we herein report the synthesis of (2E)-2-(acetylamino)-3-(4-nitrophenyl)prop-2-enoic acid (NPP) having an LD_{50} value of 2400 mg/kg (oral, rat). This study aims to evaluate the inhibition efficiency of NPP and perform its comparison with the parent compound 4-nitrobenzaldehyde (NB) on the corrosion of mild steel in 1M hydrochloric acid solution. The investigation was performed using various methods: absorbance difference measurements, potentiodynamic polarization, and electrochemical impedance spectroscopy (EIS). Also, scanning electron microscopy (SEM) and energy dispersive X-ray (EDX) was applied for the mild steel used. Besides, quantum chemical calculations were carried out to clarify the effect of these molecules and their electronic properties in inhibition efficiency.

2. Experimental

2.1 *Synthesis procedure of NPP inhibitor*

The synthesis of the NPP inhibitor is schematically displayed in Scheme 1. The structures and the IUPAC names of NPP and NB inhibitors are given in Table S1 (Supplementary Information).

Part 1- Azlactone synthesis

A mixture of 58.5 g (0.5 mol) of acetylglycine, 30 g (0.37 mol) of anhydrous sodium acetate, 111 g (0.74 mol) of freshly distilled para-nitrobenzaldehyde and 134 g (1.25 mol) of 95% acetic anhydride in a 1L round-bottomed flask and boiled for one hour under reflux, cooled and placed in a refrigerator overnight. The solid mass of yellow crystals was treated with 125 mL of cold water. The crystals were then transferred to a Büchner funnel and washed thoroughly with cold water then dried in a vacuum desiccator over phosphorus pentoxide. The yield of crude azlactone was about 75% and was sufficiently pure for the next step.

Part 2-Azlactone opening

In a 1L round-bottom flask, 58 g (0.25 mol) of the crude azlactone was dissolved by boiling with a mixture of 450 mL of acetone and 175 mL of water. Hydrolysis was completed by boiling under reflux for four hours. Most of the acetone was then removed by distillation. The residual solution was diluted with 400 mL of water, heated to boiling for five minutes to ensure the complete solution of the acetamino acid and filtered. After standing in a refrigerator overnight, the colorless crystalline needles were collected on a Büchner funnel, washed with 150–200 mL of ice-cold water and dried for several hours at 90–100°C. The yield of the purified product was 80%. The FTIR spectrum of NPP shown in Figure S1 (Supplementary Information).

(2E)-2-(acetylamino)-3-(4-nitrophenyl)prop-2-enoic acid (NPP)

^{13}C-NMR (75.47 MHz; $CDCl_3$) δ (ppm) = 166.1 (C=O), 152.6(–C=N), 144.2 (=C–N–), 133.2, 132.1, 128.6 (2C), 127.2 (2C) (C_6H_5 aromatic carbons), 114.0 (–C=C methylidene),17.2 ($\underline{C}H_3$) Figure S2 (Supplementary Information).

^{1}H-NMR (Bruker, 300.13 MHz, $CDCl_3$) δ (ppm) = 3.09 (s, 3H, CH_3), 6.7(d, 2H, H_{arom}(^{3}J = 8.9 Hz)), 7.75(d, 2H, H_{arom} (^{3}J = 8.9Hz)), 9.7 (s, 1H, HC=) Figure S3 (Supplementary Information).

2.2 *Materials preparation*

The material used in this work is mild steel with the following chemical composition: Fe (99.21), C (0.21), Mn (0.05), Si (0.38), S (0.05), P (0.09) and Al (0.01). The mild steel surface was polished with emery paper (until 1500 grit size), washed with distilled water, degreased by acetone and dried before the start of each experiment used in this study. The hydrochloric acid solution (1M) was prepared by dilution of analytical grade 37% HCl. The concentration range of the studied inhibitors was 10^{-3}M–10^{-6}M.

2.3 *Absorbance difference measurements*

The absorbance difference measurements were performed, as Alfred Onen et al. mentioned in his article.[14] Firstly, the samples were immersed in the aggressive solution 1M HCl without and with varying inhibitor concentration and placed in a thermostated water bath at 298K for 6 h. The absorbance of these solutions was taken at a wavelength of 480 nm using UV/Visible spectrophotometer (UV-6300PC, Double Beam Spectrophotometer). The difference between (A_0) and (A_1) was recorded as the absorbance difference of the corroding in each case. All the reported readings are the median of five experimental readings. The inhibition efficiency (%IE) of (NB) and (NPP) inhibitors was calculated using the relation:

$$IE_{abs}\,(\%) = \frac{A' - A}{A'} \times 100 \qquad (1)$$

where (A°) and (A) are absorbance for steel in the absence and presence of inhibitors in 1M HCl solution at 298K.

2.4 *Electrochemical studies*

The electrochemical tests were performed using potentiostat Tacussel-Radiometer PGZ 100 controlled with software analysis Volta Master 4. The various electrochemical experiments were conducted using a three-electrode glass

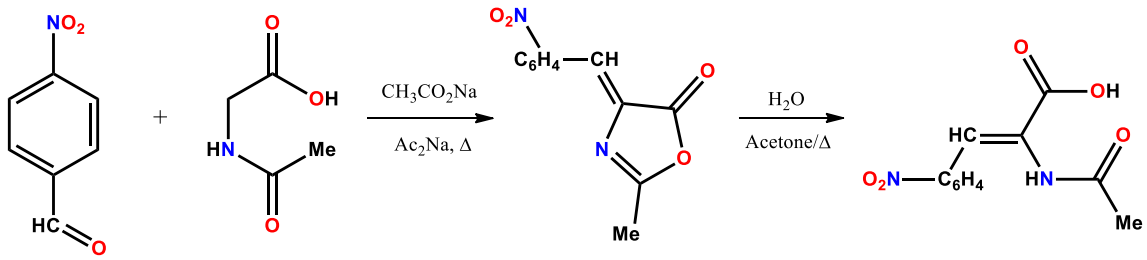

Scheme 1. Synthesis procedure of NPP inhibitor.

cell. Platinum as the counter electrode, Ag/AgCl as a reference electrode, and mild steel as the working electrode were used. Before the experiments, the potential of the working electrode was stabilized for 30 min to achieve a stable open circuit potential. The polarization curves were realized at a scan rate of 1 mV/s. The EIS tests were recorded in a frequency range from 100 KHz to 100 mHz with 10 points per decade.

2.5 *Surface analysis*

The scanning electron microscopy (SEM) is an excellent method for surface morphology analysis of metallic samples in corrosion studies. This technique can confirm the higher protective behavior of the studied inhibitors. The SEM technique was performed after an immersion of 6 h in the presence and absence of NPP and NB inhibitors at an optimum concentration of 10^{-3}M. The material composition is obtained using EDX attached to the scanning electron microscopy with an acceleration voltage of 20 kV.

2.6 *Theoretical studies*

Quantum chemical calculations can provide a lot of information about structural properties, and correlate the capability of adsorption of corrosion inhibitors with their structural aspects. The reactivity descriptors such as the highest occupied molecular orbital (HOMO), lowest unoccupied molecular orbital (LUMO), dipole moment (μ), and the energy gap (ΔE_{gap}), etc. were evaluated in the current study. Also, the reactive sites from electrophile or nucleophile attacks were extracted using Fukui indices calculations. These calculations were executed with Gaussian 09 program package[15,16] using DFT/ (B3LYP) with a basis set 6-31G (d,p).

3. Results and Discussion

3.1 *Absorbance difference measurements*

3.1a *Effect of concentration*: The inhibition efficiencies for mild steel at different concentrations of benzaldehyde derivatives in 1M hydrochloric solution at 298K obtained from absorbance difference measurements are given in Table S2 (Supplementary Information). The absorbance difference results indicate that the inhibition effect of NPP and NB increases with concentration to attain a maximum percentage of 93% and 84% at optimal concentration, respectively. This result reflects the ability of our inhibitors to adsorb on the mild steel surface through the substituent groups,[8] heteroatoms and the delocalized π electrons in the aromatic ring of benzaldehyde derivatives and the vacant d-orbital of mild steel surface.[9]

3.2 *Polarization curves*

3.2a *Effect of concentration*: The polarization curves of mild steel in 1M HCl media obtained with and without various concentrations of NPP and NB are illustrated in Figure 1. The electrochemical parameters such as I_{corr}, $E_{coor,}$ and Tafel slopes (ßc, ßa) were extracted by the extrapolation of Tafel curves (Table 1). The inhibition efficiency (IE_{pol} %) was calculated using equation Eq. 2:[17,18]

$$IE_{Pol}\,(\%) = \frac{i_{corr} - i'_{corr}}{i_{corr}} \qquad (2)$$

where i_{corr} and i'_{corr} are the corrosion current densities without and in the presence of inhibitors, respectively.

The polarization results indicate that the corrosion current densities (i_{corr}) decrease with the increase with the benzaldehyde derivatives concentration. Also, the inhibition efficiency increases by the addition of inhibitors to achieve maximum values of 94% and 84% for NPP and NB, respectively. On the other side, the cathodic Tafel slopes decreased with the same trend, which suggests that no modification can be observed for hydrogen evolution mechanism in the studied surface area.[19,20] Many researchers have suggested that the displacement of E_{corr} of inhibitor

compared to that of blank potential is an indication about the classification of the studied inhibitors. The inhibitor can be termed as cathodic or anodic inhibitor when the displacement of E_{corr} is more than ~85 mV; if not, it is a mixed type inhibitor.[20] In our study, it can be suggested that the NPP and the NB inhibitors can be considered as mixed-type inhibitors with predominantly anodic nature since the displacement of E_{corr} value is less than 85mV.

3.2b *Effect of temperature*: In the corrosion study, the effect of temperature is very important because an increase in temperature can accelerate the dissolution of materials, and modifies the kinetics of the reactions.[19–21] Therefore, it is necessary to test the inhibition efficiency of these inhibitors at different temperatures. The polarization curves in 1M of the hydrochloric acid solution obtained at the optimum concentration of the studied inhibitors at various temperatures are presented in Figure S4 (Supplementary Information).

It can be seen from Table S3 (Supplementary Information) that the current density in the presence of inhibitors concentration is less than those obtained in the blank solution indicating the adsorption behavior of our molecules. Also, it shows a minimum variation in the inhibition efficiency with the rise of temperature from 298K to 328K. Consequently, it can be suggested that these inhibitors act by chemical adsorption.

3.2c *Activation parameters*: Thermodynamic activation parameters of mild steel in acidic medium calculated through Arrhenius equations Eqs. 3 and 4[22,23]:

$$i_{corr} = Ae^{\frac{-E_a}{RT}} \tag{3}$$

$$i_{corr} = \frac{RT}{NH} e^{\left(\frac{\Delta S}{R}\right)} e^{\left(-\frac{\Delta H}{RT}\right)} \tag{4}$$

where R is the universal gas constant, A is Arrhenius factor, T is the absolute temperature, N is Avogadro's number, h is Planck's constant (h = 6.6252 10^{-34} J s), ΔH*, ΔS* and E_a are enthalpy, entropy, and activation energy, respectively.

From the results shown Figure 2 and the data in Table S4 (Supplementary Information), it can be concluded that the values for the enthalpy of activation ΔH* in the inhibited medium are higher than those obtained in uninhibited solution. This means that the dissolution of steel is slow in the presence of the benzaldehyde derivatives, especially for NPP inhibitor, confirming the higher inhibition effect of this compound compared to NB. Moreover, the activation energy values are greater compared to the blank solution, which indicates that the inhibitors adsorb on the steel surface by physical adsorption.

3.3 *Electrochemical impedance results*

Electrochemical impedance spectroscopy (EIS) is an effective method for corrosion studies.[24,25] The inhibition effect of NPP and NB was also evaluated by this technique. The impedance parameters obtained in the presence and absence of inhibitors at different concentrations in acidic medium was extracted after a good fitting and regrouped in Table 2. The Nyquist plots for the mild steel surface obtained at 298K with and without inhibitors are presented in Figure 3.

The appearance of depressed semicircles in the Nyquist plots of Figure 3 show that the electrochemical process of corrosion is charge transfer controlled.[26–28] It can be seen from the data of Table 2 that NPP inhibitor shows superior performance compared to NB inhibitor. This performance may be explained by the condensation between 4-nitrobenzaldehyde and (acetylamino) acetic acid.[21] On the other hand, the charge transfer resistance R_t increases slightly with inhibitor concentration while the double layer capacitance C_{dl} decreases. These results indicate that our inhibitor compounds adsorb on the mild steel surface forming a protective layer.[11,29,30]

The values of the factor of heterogeneity n_{dl} increases with the concentration of inhibitors due to a reduction in the heterogeneities of the mild steel surface against the aggressive medium.[31] The equivalent circuit (Inset to Figure 3) model used in this study contained the constant phase element Q in the place of capacitor in order to achieve an appropriate simulation since the Nyquist plots are not perfect.[32,33] The depressed semicircles appear due to the frequency distribution, occurring due to surface inhomogeneity, occurring due to corrosion damage. The circuit diagram used is the modified Randle's circuit wherein instead of the ideal double-layer capacitor, we have used a constant phase element to model the frequency dispersion behavior.[21] The inhibition efficiency of benzaldehyde derivatives tested showed the same trend in all the techniques used.

In order to find that the three methods show a good correlation, a histogram (Figure S5, Supplementary Information) was constructed to compare the inhibition efficiency values obtained at 10^{-3}M of NPP and NB inhibitors by the different methods tested in this study. The result indicates that all the methods

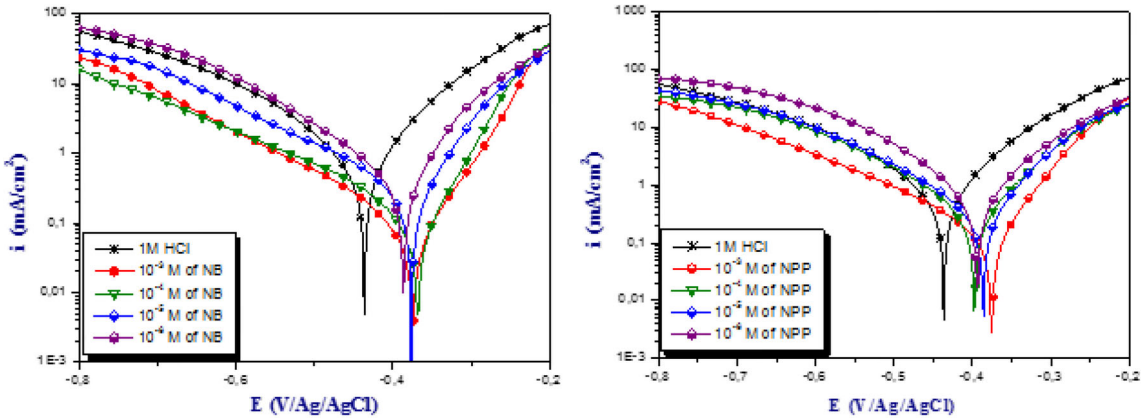

Figure 1. Polarization curves for mild steel in acidic medium without and with the addition of NPP and NB at different concentrations of inhibitors at 298K.

Table 1. Electrochemical polarization parameters for mild steel in 1M HCl with different concentrations of inhibitors at 298K.

Medium	Conc. (M)	$-E_{corr}$ (mV/Ag/AgCl)	i_{corr} (μA cm^{-2})	$-\beta_c$ (mV dec^{-1})	β_a (mV dec^{-1})	IE (%)
1M HCl	**	437	983	140	150	**
NPP	10^{-6}	367	605	134	69	38
	10^{-5}	376	283	130	66	71
	10^{-4}	368	113	124	57	89
	10^{-3}	375	62	92	62	94
NB	10^{-6}	393	682	143	120	31
	10^{-5}	386	465	137	82	53
	10^{-4}	397	356	134	94	64
	10^{-3}	374	160	131	61	84

(absorbance difference, polarization curves and EIS) confirm that the synthetic product acts as good inhibitor of mild steel corrosion in 1M HCl. Also, the difference between the three methods is not significant because we have the same trend for all values of the inhibition efficiency (IE%).

3.4 *Adsorption behavior*

In order to find information about the adsorption mechanism of inhibitors, it is necessary to examine the different models of isotherms. For this reason, the experimental results of impedance measurements were tested with different adsorption isotherms: Freundlich, El-Awady, Frumkin, Flory-Huggins and Temkin. We used the following linear equations of the various isotherms.[1] The Linear equations for the different used isotherms are provided in Table S5 (Supplementary Information). The plots of the tested adsorption isotherms are given in Figure S6 and the obtained parameters are given in Table S6 (Supplementary Information).

The examination of the tested isotherm models shows that one active site can adsorb more than one molecule of water. The adsorption constant obtained from Freundlich isotherm has not significance despite that the correlation coefficient is close to unity. Also, the parameter Z of Freundlich isotherm is far from the typical value of 0.6.[34] Moreover, the data obtained from El-Awady isotherm[35] is compatible for NB inhibitor since it shows a more appropriate value of the coefficient of regression compared to the other models traced. From these results, it can be suggested that one molecule of NB inhibitor can displace three molecules of water. Furthermore, the value of standard Gibbs free energy (ΔG^0_{ads}) indicates that NB shows mixed adsorption (physical and chemical adsorption), the electrostatic bonds may be formed due to nitro-substitution of NB. On the other hand, the adsorption behavior for NPP inhibitor shows that the good coefficient of a linear regression of isotherms tested obtained from Temkin isotherm, the negative value of parameter (A) reflects the attraction interaction in the adsorbed layer.[36] This result was also obtained by Frumkin isotherm. The values of standard free energy

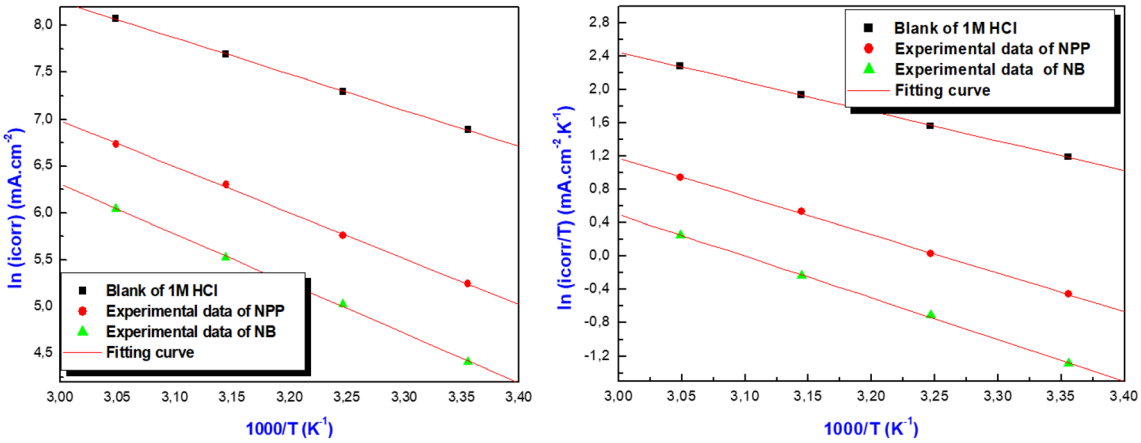

Figure 2. Arrhenius plots of mild steel in 1M HCl at 10^{-3}M of inhibitors.

indicate that NPP inhibitor adsorbs on the surface of mild steel forming coordination bonds (chemical adsorption).

3.5 *Surface analysis*

SEM studies of the mild steel surfaces were also carried out with and without inhibitors after a 6 h immersion period at 298 K. SEM micrographs are shown in Figure S7 (Supplementary Information). The morphology of mild steel before immersion is smoother compared to the blank (after immersion in acidic solution), the surface in 1M HCl was too damaged, which is explained by the metal dissolution upon penetration of the acidic solution (Figure S7 (a) (b), Supplementary Information).[26,29] While, the presence of NB and NPP inhibitors shows the formation of a heterogeneous protective film indicating the adsorption of tested inhibitors on the steel surface (Figure S7 (c) (d), Supplementary Information).

Energy-dispersive X-ray analysis (EDX) method was also used in order to get the composition of the element adsorbed on the surface of mild steel without and with the inhibitors. The results shown in Figure S8 (Supplementary Information) revealed the presence of heteroatoms such as nitrogen and oxygen explaining the adsorption of the studied corrosion inhibitors onto the steel surface. The percentage atomic content of the different elements obtained by EDX analysis is illustrated in Table S7 (Supplementary Information). The results show that NPP inhibitor protects the mild steel surface more than the NB inhibitor since the percentage of nitrogen atom is higher than that obtained in NB inhibitor. On the other hand, the percentage of Cl and the Fe atoms were less than that obtained in 1M HCl indicating the adsorption behavior of the studied compounds.

3.6 *Theoretical study*

3.6a *Global molecular reactivity of NPP and NB inhibitors*: Generally, the higher inhibition efficiency depends on the nature of molecules studied. To get information about reactivity of our inhibitors and to

Table 2. Impedance results of mild steel in molar hydrochloric acid with and without inhibitors at different concentrations at 298K.

Medium	Conc. (M)	R_s (Ω cm^2)	R_{ct} (Ω cm^2)	Q (μF Sn^{-1})	n_{dl}	C_{dl} (μF cm^{-2})	IE (%)
1M HCl	**	1.12	34,7	315.0	0.770	121.0	**
NPP	10^{-6}	1.60	54.4	257.4	0.764	69.02	36.2
	10^{-5}	1.50	116.7	159.3	0.762	45.98	70.2
	10^{-4}	1.59	256.3	161.7	0.732	50.59	86.5
	10^{-3}	1.66	362.1	70.93	0.792	27.21	90.4
NB	10^{-6}	1.20	49.2	282.2	0.736	60.97	29.5
	10^{-5}	2.08	69.8	244.4	0.754	64.95	50.3
	10^{-4}	2.29	88.0	195.2	0.765	56.1	60.5
	10^{-3}	1.55	181.6	123.7	0.774	40.99	80.9

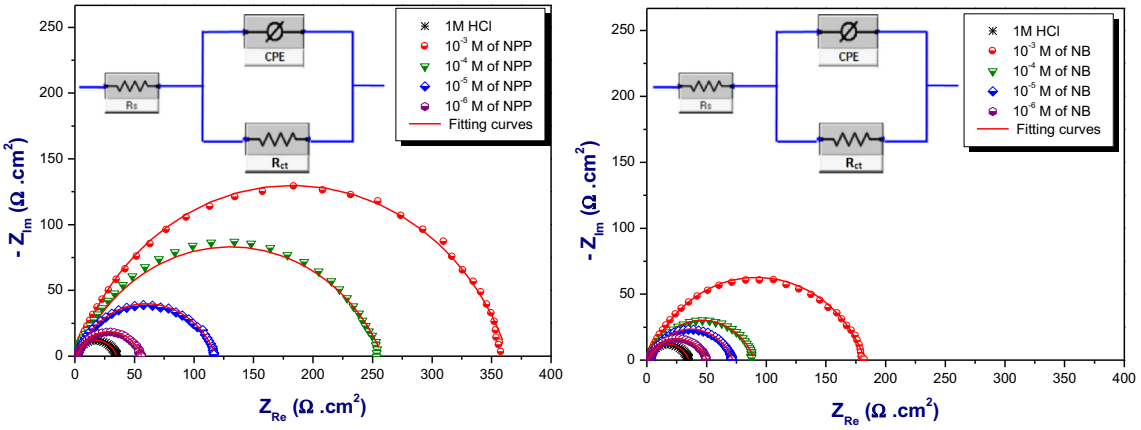

Figure 3. Nyquist plots for benzaldehyde derivatives in 298K at various concentrations. Inset shows the equivalent circuit used in EIS data.

Table 3. Quantum descriptors of the studied inhibitors.

Inhibitors	NPP	NB
E_{HOMO} (eV)	− 6.3642	− 10.6034
E_{LUMO} (eV)	− 2.8505	− 0.1705
I (eV)	6.3642	10.6034
A (eV)	2.8505	0.1705
η	4.9389	10.5181
σ	0.2024	0.0950
ΔN	1.2702	0.8408
X	− 10.9691	− 10.6886
ΔE (eV)	2.4611	2.6150
μ(D)	0.9706	3.7300
Total energy (u.a)	− 910.7641	− 543.7802
IE (%) (EIS)	94	84

justify the order of their inhibition efficiency obtained in the experimental part, different descriptors were calculated such as:[37,38] energy gap (ΔE), dipole moment (μ), ionization potential (I), electronegativity (χ), global hardness (η), softness (σ), electron affinity (A) and the fraction of electrons transferred (ΔN) using the following equations and are given in Table 3:[1]

$$\Delta E = E_{LUMO} - E_{HOMO} \tag{5}$$

$$I = -E_{HOMO} \tag{6}$$

$$A = -E_{LUMO} \tag{7}$$

$$\chi = -\frac{1}{2}(E_{LUMO} + E_{HOMO}) \tag{8}$$

$$\eta = -\frac{1}{2}(E_{HOMO} - E_{LUMO}) \tag{9}$$

$$\sigma = \frac{1}{\eta} \tag{10}$$

$$\Delta N = \frac{\chi_{metal} - \chi_{inh}}{2(\eta_{metal} + \eta_{inh})} \tag{11}$$

Firstly, the NPP inhibitor possesses the lowest value of $E_{LUMO,}$ indicating the higher capacity of this molecule to accept electrons.[19,39] However, NPP inhibitor has the smallest energy gap (ΔE) compared to NB, which might provide a higher reactivity to the NB inhibitors,[40] as a result of the lower excitation energy from the last occupied orbital.[41] Moreover, according to Lukovits, the value of the fraction of electrons transferred (ΔN) is less than 3.6, which reflects the electron-transfer capability to the metal surface.[42] Also, the dipole moment shows the same trend as the inhibition efficiency. These theoretical results show a better correlation with those obtained experimentally.

Figure 4 shows that the HOMO and LUMO electron density of the studied benzaldehyde derivatives studied (NPP and NB) concentrated around aromatic ring reflecting the capability of these inhibitors to exchange electrons with the metal surface. Therefore, the adsorption behavior is probably going to occur on reactive sites of the inhibitor molecules.

3.6b *Local molecular reactivity of NPP and NB inhibitors in the aqueous medium*: From the natural populations for atoms in different states anionic, cationic, and neutral species. Fukui indices were computed to find the available information about the active sites for nucleophilic or electrophilic attacks of these inhibitor molecules. These indices were calculated from the following equations:[11,43]

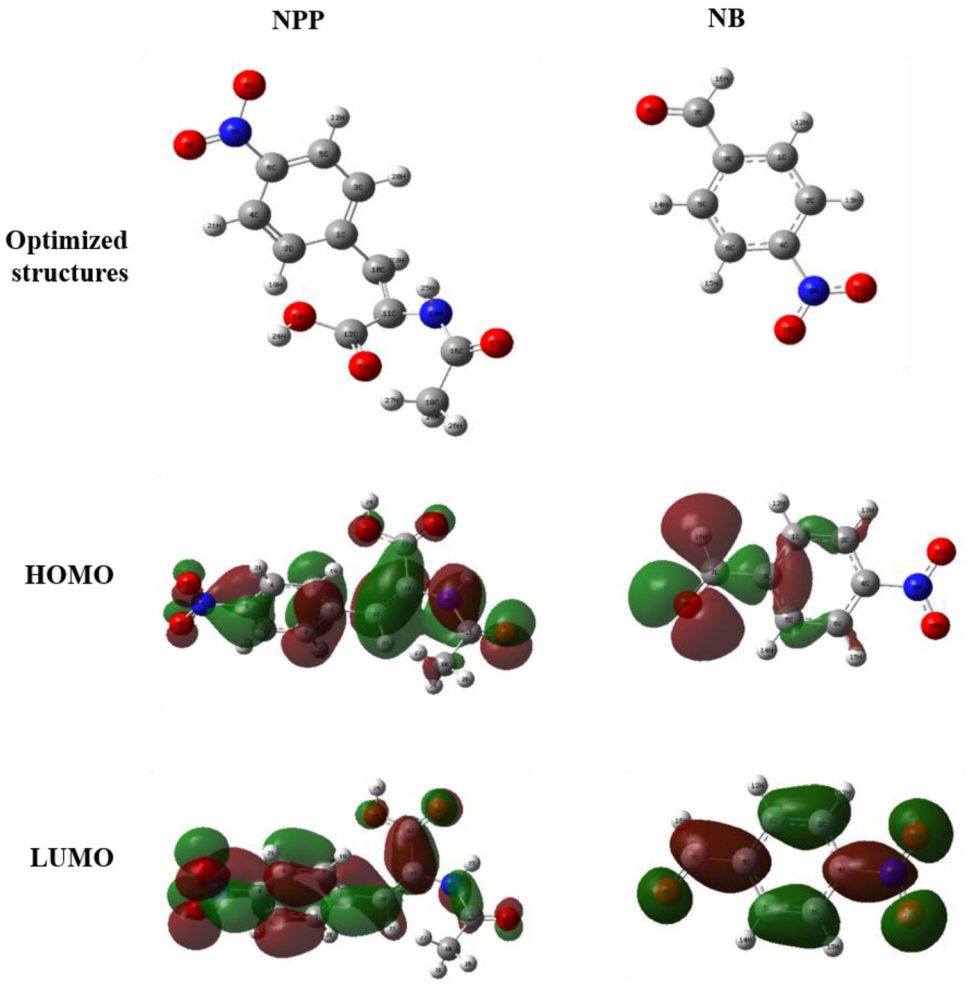

Figure 4. Geometry optimization and Electron density distributions (HOMO & LUMO) of NPP and NB inhibitors obtained by B3LYP/6-31G (d,p) level.

$$\mathbf{F_k^+ = P_k(N+1) - P_k(N)} \quad (11)$$

$$\mathbf{F_k^- = P_k(N) - P_k(N-1)} \quad (13)$$

$$\mathbf{F^0 = P_k(N+1) - P_k(N-1)} \quad (14)$$

where $P_K(N)$, $P_K(N + 1)$, and $P_K(N - 1)$ are the natural populations for the atom k in the neutral, anionic and cationic species, respectively.

From the results shown in Table S8 (Supplementary Information), the most probable sites for nucleophilic or electrophilic attacks of inhibitor molecules indicate that the reactive sites on NB inhibitor are localized only on N9, C7 and C4 atoms. While the NPP inhibitor possesses various active sites throughout the whole molecule structure, which can explain the higher protective behavior compared to NB inhibitor.

4. Conclusions

The studied inhibitors (NPP and NB) show an excellent performance against corrosion of mild steel in hydrochloric acid solution and confirmed by different techniques. The result obtained experimentally has a good correlation with theoretical calculations. From these results, we can conclude that:

- The polarization curves indicate that our compounds can be classified as mixed-type inhibitors.
- The electrochemical impedance spectroscopy indicates that the inhibition efficiencies attain a maximum value of 94% and 84% for NPP and NB, respectively.
- The variation of inhibition efficiency with temperature has no significant effect but increases slightly with inhibitor concentration.

- The adsorption behavior shows that one molecule of the inhibitor can remove three water molecules, according to El-Awady isotherm.
- The surface morphology studies show that the inhibitor compounds form a protective film on the surface of mild steel.
- The global and selective descriptors obtained are in good correlation with the experimental part.

Supplementary Information (SI)

Figures S1–S8 and Tables S1–S8 are available at www.ias.ac.in/chemsci.

References

1. Quraishi M A, Chauhan D S and Saji V S 2020 *Heterocyclic Corrosion Inhibitors: Principles and Applications* (Amsterdam: Elsevier Inc.)
2. Sastri V S 1998 *Corrosion Inhibitors: Principles and Applications* (New York: Wiley)
3. El-Hajjaji F, Messali M, de Yuso M M, Rodríguez-Castellón E, Almutairi S, Bandosz T J and Algarra M 2019 Effect of 1-(3-phenoxypropyl) pyridazin-1-ium bromide on steel corrosion inhibition in acidic medium *J. Colloid Interface Sci.* **541** 418
4. Salim R, Ech-chihbi E, Oudda H, El Hajjaji F, Taleb M and Jodeh S 2019 A review on the assessment of imidazole [1,2-a] pyridines as corrosion inhibitor of metals *J. Bio Tribo Corros.* **13** 5
5. Saady A, El-Hajjaji F, Taleb M, Alaoui K I, El Biache A, Mahfoud A, Alhouari G, Hammouti B, Chauhan D S and Quraishi M A 2018 Experimental and theoretical tools for corrosion inhibition study of mild steel in aqueous hydrochloric acid solution by new indanones derivatives *Mater. Discov.* **12** 30
6. Sastri V S 2012 *Green Corrosion Inhibitors: Theory and Practice* (New York: Wiley)
7. Pournazari S, Moayed M H and Rahimizadeh M 2013 In situ inhibitor synthesis from admixture of benzaldehyde and benzene-1, 2-diamine along with $FeCl_3$ catalyst as a new corrosion inhibitor for mild steel in 0.5 M sulphuric acid *Corros. Sci.* **71** 20
8. Singh D K, Kumar S, Udayabhanu G and John R P 2016 4 (N, N-dimethylamino) benzaldehyde nicotinic hydrazone as corrosion inhibitor for mild steel in 1 M HCl solution: an experimental and theoretical study *J. Mol. Liq.* **216** 738
9. Zhang H and Chen Y 2019 Experimental and theoretical studies of benzaldehyde thiosemicarbazone derivatives as corrosion inhibitors for mild steel in acid media *J. Mol. Struct.* **1177** 90
10. Ansari K R, Chauhan D S, Quraishi M A, Mazumder M A and Singh A 2020 Chitosan Schiff base: an environmentally benign biological macromolecule as a new corrosion inhibitor for oil & gas industries *Int. J. Biol. Macromol.* **144** 305
11. Chauhan D S, Quraishi M A, Sorour A, Saha S K and Banerjee P 2019 Triazole-modified chitosan: a biomacromolecule as a new environmentally benign corrosion inhibitor for carbon steel in a hydrochloric acid solution *RSC Adv.* **9** 14990
12. Verma C, Ebenso E E, Bahadur I and Quraishi M A 2018 An overview on plant extracts as environmental sustainable and green corrosion inhibitors for metals and alloys in aggressive corrosive media *J. Mol. Liq.* **266** 577
13. Verma C, Ebenso E E and Quraishi M A 2017 Ionic liquids as green and sustainable corrosion inhibitors for metals and alloys: an overview *J. Mol. Liq.* **233** 403
14. Onen A I, Nwufo B, Ebenso E E and Hlophe R M 2010 Titanium (IV) oxide as corrosion inhibitor for aluminium and mild steel in acidic medium *Int. J. Electrochem. Sci.* **5** 1563
15. Dennington R, Keith T, Millam J 2009 GaussView, version 5, Semichem Inc.: Shawnee Mission, KS.
16. Frisch M, Trucks G, Schlegel H B, Scuseria G, Robb M, Cheeseman J, Scalmani G, Barone V, Mennucci B and Petersson G 2009, Gaussian 09, revision a. 02, Gaussian, Inc., Wallingford, CT, 200.
17. Frankel G S and Rohwerder M 2007 *Electrochemical techniques for corrosion* Encyclopedia of Electrochemistry A J Bard (Ed.). (Wiley)
18. McCafferty E 2005 Validation of corrosion rates measured by the Tafel extrapolation method *Corros. Sci.* **47** 3202
19. Baig N, Chauhan D S, Saleh T A and Quraishi M A 2019 Diethylenetriamine functionalized graphene oxide as a novel corrosion inhibitor for mild steel in hydrochloric acid solutions *New J. Chem.* **43** 2328
20. El-Hajjaji F, Messali M, Aljuhani A, Aouad M, Hammouti B, Belghiti M, Chauhan D S and Quraishi M A 2018 Pyridazinium-based ionic liquids as novel and green corrosion inhibitors of carbon steel in acid medium: Electrochemical and molecular dynamics simulation studies *J. Mol. Liq.* **249** 997
21. Singh P, Chauhan D S, Chauhan S S, Singh G and Quraishi M A 2019 Bioinspired synergistic formulation from dihydropyrimdinones and iodide ions for corrosion inhibition of carbon steel in sulphuric acid *J. Mol. Liq.* **298** 112051
22. Alvarez P E, Fiori-Bimbi M V, Neske A, Brandán S A and Gervasi C A 2018 Rollinia occidentalis extract as green corrosion inhibitor for carbon steel in HCl solution *J. Industr. Eng. Chem.* **58** 92
23. Oguzie E, Okolue B, Ebenso E, Onuoha G and Onuchukwu A 2004 Evaluation of the inhibitory effect of methylene blue dye on the corrosion of aluminium in hydrochloric acid *Mater. Chem. Phys.* **87** 394
24. El Hajjaji F, Salim R, Messali M, Hammouti B, Chauhan D S, Almutairi S and Quraishi M A 2019 Electrochemical studies on new pyridazinium derivatives as corrosion inhibitors of carbon steel in acidic medium *J. Bio Tribo Corros.* **5** 4
25. El Hajjaji F, Abrigach F, Hamed O, Hasan A R, Taleb M, Jodeh S, Rodríguez-Castellón E, del Valle Martínez de Yuso M and Algarra M 2018 Corrosion resistance of mild steel coated with orgainc material containing pyrazol moiety *Coatings* **8** 330

26. Chauhan D S, Mouaden K E, Quraishi M A and Bazzi L 2020 Aminotriazolethiol-functionalized chitosan as a macromolecule-based bioinspired corrosion inhibitor for surface protection of stainless steel in 3.5% NaCl *Int. J. Biol. Macromol.* **152** 234
27. Chauhan D S, Quraishi M A, Carrière C, Seyeux A, Marcus P and Singh A 2019 Electrochemical, ToF-SIMS and computational studies of 4-amino-5-methyl-4H-1, 2, 4-triazole-3-thiol as a novel corrosion inhibitor for copper in 3.5% NaCl *J. Mol. Liq.* **289** 111113
28. Chauhan D S, Kumar A M and Quraishi M A 2019 Hexamethylenediamine functionalized glucose as a new and environmentally benign corrosion inhibitor for copper *Chem. Eng. Res. Des.* **150** 99
29. Chauhan D S, Ansari K R, Sorour A, Quraishi M A, Lgaz H and Salghi R 2018 Thiosemicarbazide and thiocarbohydrazide functionalized chitosan as eco-friendly corrosion inhibitors for carbon steel in hydrochloric acid solution *Int. J. Biol. Macromol.* **107** 1747
30. Chauhan D S, Srivastava V, Joshi P G and Quraishi M A 2018 PEG cross-linked chitosan: a biomacromolecule as corrosion inhibitor for sugar industry *Int. J. Indus. Chem.* **9** 363
31. Yadav D K, Chauhan D S, Ahamad I and Quraishi M A 2013 Electrochemical behavior of steel/acid interface: adsorption and inhibition effect of oligomeric aniline *RSC Adv.* **3** 632
32. Sudheer M and Quraishi M A 2013 Electrochemical and theoretical investigation of triazole derivatives on corrosion inhibition behavior of copper in hydrochloric acid medium *Corros. Sci.* **70** 161
33. Sudeer M and Quraishi M A 2015 The corrosion inhibition effect of aryl pyrazolo pyridines on copper in hydrochloric acid system: computational and electrochemical studies *RSC Adv.* **5** 41923
34. Fu J, Pan J, Liu Z, Li S and Wang Y 2011 Corrosion inhibition of mild steel by benzopyranone derivative in 1.0 M HCl solutions *Int. J. Electrochem. Sci.* **6** 2072
35. Gerengi H, Mielniczek M, Gece G k and Solomon M M 2016 Experimental and quantum chemical evaluation of 8-hydroxyquinoline as a corrosion inhibitor for copper in 0.1 M HCl *Industr. Eng. Chem. Res.* **55** 9614
36. Ech-chihbi E, Nahlé A, Salim R, Oudda H, El Hajjaji F, El Kalai F, El Aatiaoui A and Taleb M 2019 An investigation into quantum chemistry and experimental evaluation of imidazopyridine derivatives as corrosion inhibitors for C-steel in acidic media *J. Bio Tribo Corros.* **5** 24
37. Obot I B, Macdonald D D and Gasem Z M 2015 Density functional theory (DFT) as a powerful tool for designing new organic corrosion inhibitors. Part 1: an overview *Corros. Sci.* **99** 1
38. Geerlings P, De Proft F and Langenaeker W 2003 Conceptual density functional theory *Chem. Rev.* **103** 1793
39. Dohare P, Chauhan D S, Sorour A and Quraishi M A 2017 DFT and experimental studies on the inhibition potentials of expired Tramadol drug on mild steel corrosion in hydrochloric acid *Mater. Discov.* **9** 30
40. Dohare P, Chauhan D S, Hammouti B and Quraishi M A 2017 Experimental and DFT investigation on the corrosion inhibition behavior of expired drug Lumerax on mild steel in hydrochloric acid *Anal. Bioanal. Electrochem.* **9** 762
41. Srivastava V, Chauhan D S, Joshi P G, Maruthapandian V, Sorour A A and Quraishi M A 2018 PEG-functionalized chitosan: A biological macromolecule as a novel corrosion inhibitor *ChemistrySelect* **3** 1990
42. Lukovits I, Kalman E and Zucchi F 2001 Corrosion inhibitors—correlation between electronic structure and efficiency *Corrosion* **57** 3
43. Singh P, Ebenso E E, Olasunkanmi L O, Obot I and Quraishi M A 2016 Electrochemical, theoretical, and surface morphological studies of corrosion inhibition effect of green naphthyridine derivatives on mild steel in hydrochloric acid *J. Phys. Chem. C* **120** 3408